

## Internal structure of the volcanic island of Surtsey and surroundings: Constraints from a dense aeromagnetic survey



Sara Sayyadi <sup>a,b,\*</sup>, Magnús T. Gudmundsson <sup>a</sup>, James D.L. White <sup>c</sup>, Thorsteinn Jónsson <sup>a</sup>, Maxwell C. Brown <sup>a,d</sup>, Marie D. Jackson <sup>e</sup>

<sup>a</sup> *Nordvulk, Institute of Earth Sciences, University of Iceland, Askja, Sturlugata 7, 102 Reykjavík, Iceland*

<sup>b</sup> *Hydrology Section, Helmholtz Centre Potsdam GFZ German Research Centre for Geosciences, Potsdam, Germany*

<sup>c</sup> *Geology Department, University of Otago, Dunedin, New Zealand*

<sup>d</sup> *Institute for Rock Magnetism, Department of Earth and Environmental Sciences, University of Minnesota, Minneapolis, MN, USA*

<sup>e</sup> *Department of Geology and Geophysics, University of Utah, Salt Lake City, UT, USA*

### ARTICLE INFO

#### Keywords:

Aeromagnetic survey

Volcanic island

Surtsey

Phreatomagmatic eruption

### ABSTRACT

Surtsey, a young basaltic island off the south coast of Iceland, was built by volcanic activity in 1963–1967 from a pre-eruption oceanic seafloor depth of 130 m. An aeromagnetic survey was carried out in October 2021 over a 60 km<sup>2</sup> area covering Surtsey and its surroundings. It aimed to explore the internal structure and the possible existence of basaltic intrusions associated with the five vents active at different times over the 3.5 years of eruptive activity. The survey line spacing was 200 m and the flying altitude was generally 90 m a.s.l. The strongest anomalies (amplitude ~700 nT) are caused by the 30–100 m thick subaerially erupted lava field on the southern part of Surtsey, formed in two episodes of effusive activity: 1964–1965 and 1966–1967. 2D spectral analysis and Euler deconvolution indicate that the causative bodies of anomalies outside the island of Surtsey are located within the uppermost 300 m of the seafloor and their horizontal dimensions are similar to or smaller than their depth. 3D forward modeling of the island and its surroundings, constrained by observations during the formation of the island and drill cores extracted in 1979 and 2017, is consistent with an absence, at all vents, of pillow lava and therefore effusive activity in their opening phases. However, the data support the existence of a 10–20 m thick pillow lava field on the seafloor, 2.5–3 km<sup>2</sup> in area, extending about ~1 km to the south of Surtsey. The field is considered to have been fed by magma reaching the seafloor via channelized intrusive flow through the foreset breccia constituting the submarine part of an emerging lava delta during the early stage of effusive eruption in May–July 1964. The general scarcity of significant magnetic bodies within the edifices is consistent with magma fragmentation dominating the submarine eruptions from the onset of activity. A small magnetic anomaly is observed over the submarine edifice of Surtla, built during short-lived activity over ~10 days in 1963–1964. This anomaly is consistent with observed subaqueous weak or moderate explosive activity that may have allowed a dyke to be preserved within the submarine tephra mound. More violent Surtseyan activity was observed at other vents, however, and may have destroyed any initial dykes that, if preserved, might have been resolved magnetically. Indications of magnetized volcanic rocks of unknown age predating the Surtsey eruption are found beneath the flank of the ephemeral island of Jónlir, the southernmost of the Surtsey vents.

### 1. Introduction

Submarine-to-emergent volcanism often leads to explosive eruptions influenced by magma–water interaction, and forms islands in the ocean and in lakes (White et al., 2015). Such eruptions can produce hazards, forming ash clouds and tephra fallout. These eruptions can also build unstable islands that abruptly collapse, causing tsunamis (e.g., Somoza

et al., 2017). Observations of eruptions in such settings inform our understanding of their style of activity, their influence on ocean waters and biota, and potential hazards. A notable example is the formation of the basaltic volcanic island of Surtsey off the south coast of Iceland in 1963–1967 (e.g., Thorarinsson et al., 1964; Thorarinsson, 1967a; Jakobsson and Moore, 1982; Moore, 1985).

Although many studies exist on subaqueous-to-emergent volcanism

\* Corresponding author at: Nordvulk, Institute of Earth Sciences, University of Iceland, Askja, Sturlugata 7, 102 Reykjavík, Iceland.

E-mail address: [sas82@hi.is](mailto:sas82@hi.is) (S. Sayyadi).

(e.g., Kokelaar, 1986; White, 1996; Cole et al., 2001; Cronin et al., 2017), it is rare that detailed observational records of eruptive activity during formation can be compared with studies of the internal structure of oceanic island volcanoes. The detailed studies that have been carried out at Surtsey, establishing the timeline of its formation (Thorarinsson,

1965, 1966, 1967a, 1968b; Baldursson and Ingadóttir, 2007) and coupling of this timeline with stratigraphic information obtained from time-lapse drill cores extracted in 1979 and in 2017 (Jakobsson and Moore, 1982; Jackson et al., 2019; Weisenberger et al., 2019) make Surtsey an ideal site for studying the internal structure of a submarine-

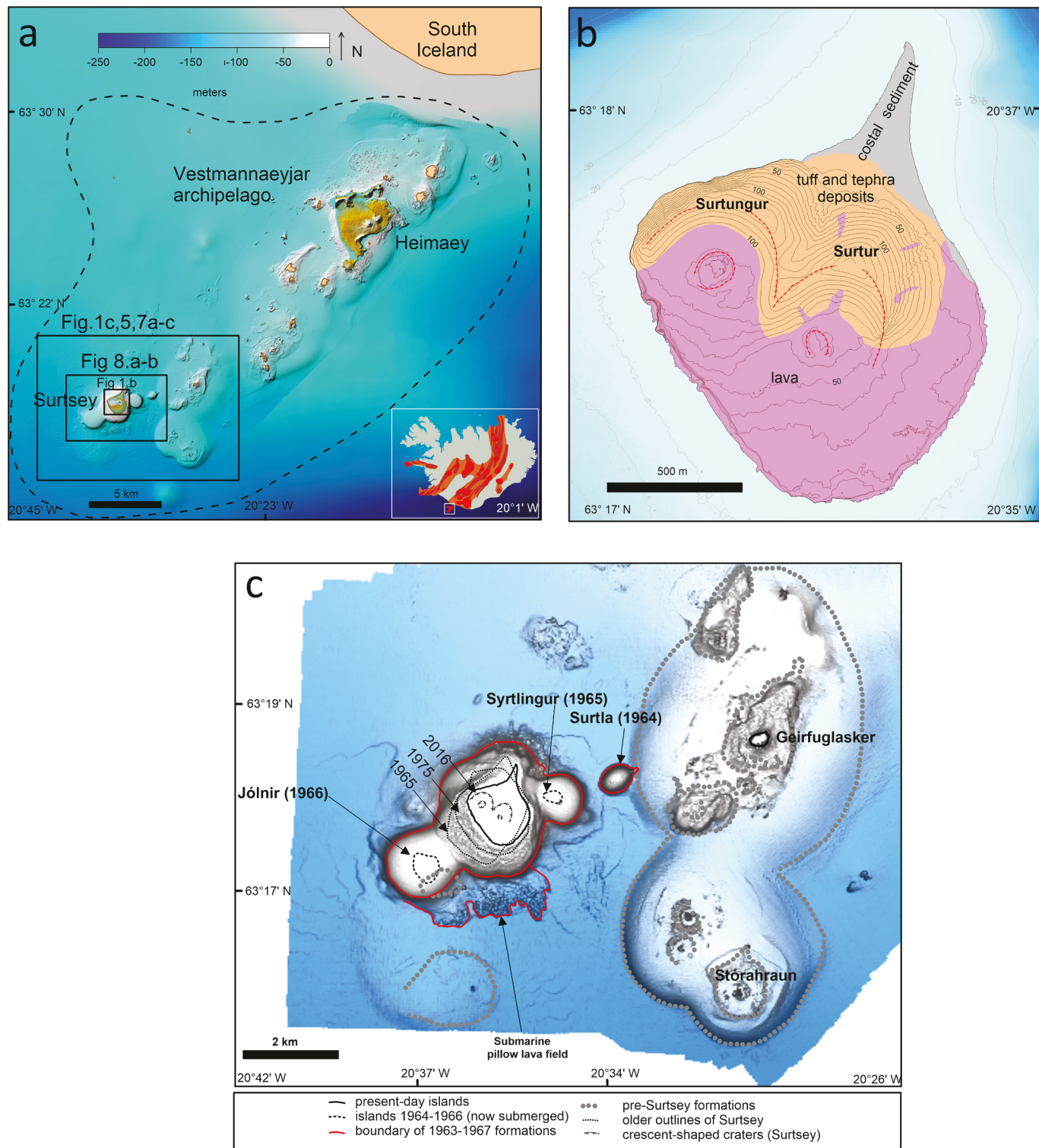


**Fig. 1.** Bathymetry of the Vestmannaeyjar archipelago. a) The black quadrangles show the outlines of the maps in Figs. 1, 5, 7, and 8. The dashed line shows the approximate outlines of the Vestmannaeyjar volcanic system. b) A geological map of Surtsey shows the location of the lava field on the southern sector of the island and the Surtungur and Surtur tuff cones formed in 1963–1964 (Jakobsson et al., 2009). c) Shaded relief bathymetry map of Surtsey and its surroundings based on a 2007 survey (Jakobsson et al., 2009). The volcanic features constructed in 1963–1967, including outlines of the ephemeral islands of Syrtlingur and Jólnir, are shown, as well as the evolving shape of the island of Surtsey since 1965. Outlines of older features of unknown age are also shown.

to-emergent monogenetic volcanic complex. Most volcanic deposits created during the 1963–1967 eruptions are submerged. This puts limits on the extent to which geological mapping can be applied to study the internal structure of the volcanic deposits. Aeromagnetic surveying, by contrast, is a method that is not hampered by the oceanic island setting. Important constraints on internal structure, intrusions, and development of other submarine volcanoes have resulted from the modeling of airborne magnetic survey data, which can be employed to image subsurface geological features (e.g., Finn and Morgan, 2002; Blanco-Montenegro et al., 2007; Okuma et al., 2009; Paoletti et al., 2009).

In October 2021, a six-hour aeromagnetic survey with a high-resolution magnetometer was completed over the Surtsey area, at the southernmost tip of the Vestmannaeyjar archipelago (Fig. 1). The main aim of the survey was to look for signs of shallow intrusions and possible pillow lava formations within and below the edifices of the Surtsey complex built in 1963–1967, as well as for any evidence of intrusions beneath the seafloor or possible signs of local tectonic structures.

A more general aim was to explore the feasibility of aeromagnetic surveying to detect remnant deposits of past eruptions in locations such as the Vestmannaeyjar archipelago, and whether magnetic surveying may provide clues on recurrence times of submarine eruptions through defining deposits of past eruptions.

## 2. Use of aeromagnetic surveying for submarine settings

Aeromagnetic surveys have been used to study diverse hydrovolcanic craters and conduits. At maars in Auckland, New Zealand, Cassidy et al. (2007) observed magnetic anomalies that were related to coherent basaltic rocks emplaced in the shallow conduits while geophysical evidence for deep diatremes was not observed beneath the two tuff cones studied. In the Izu-Oshima volcano, Japan (Ueda, 2007), the comparison of 3D magnetic models of two surveys in 1986 and 1997 illustrates a shift in the location of vents within the volcanic edifice and the ridge spreading system. A 1993 aeromagnetic survey of the Canary archipelago, Spain, analyzed by Blanco-Montenegro et al. (2020) with 3D inversion modeling, provided new insights into intrusions associated with the tectonic framework underlying the substructure of the submarine sector of the archipelago.

Aeromagnetic surveys are a cost-effective method to study offshore volcanic areas, allowing for coverage of large and inaccessible mostly submarine volcanoes. At Nishinoshima volcano, Japan, for example, constraints were obtained on volcanic processes occurring during island formation (Tada et al., 2021). A comparison of results from two aeromagnetic surveys in 2018 and 2019 revealed two newly formed shallow bodies, with their magnetization emerging in the period between the surveys, interpreted to indicate the recent emplacement of magma and its subsequent cooling beneath the crater (Tada et al., 2021).

## 3. Regional setting: the Vestmannaeyjar archipelago

The Vestmannaeyjar archipelago, composed of at least 17 islands off the south coast of mainland Iceland, is an early-stage volcanic system, with an area of  $800 \text{ km}^2$  (Fig. 1). It can be categorized as a monogenetic volcanic field (e.g., Walker, 2000; Mattsson and Hoskuldsson, 2003). The geological record indicates that over the last few tens of thousands of years, numerous eruptions have taken place, as demonstrated by several tens of remnants of submarine and subaerial vents spread over an area  $\sim 40 \text{ km}$  long (SW-NE) and  $30\text{--}35 \text{ km}$  wide (NW-SE) (Jakobsson, 1979; Mattsson and Hoskuldsson, 2003; Sigurdsson and Jakobsson, 2006). Compared to more productive volcanic systems in Iceland, the Vestmannaeyjar system is not very active, with the eruptions in Surtsey in 1963–1967 and Heimaey in 1973 the only confirmed eruptions for 1000 years (Thorarinsson et al., 1964; Hoskuldsson et al., 2015). Episodes of volcanic activity also occurred in early Holocene time and during the last glacial period ( $100 \text{ kyr}$ ) (e.g., Jakobsson, 1979; Mattsson and Hoskuldsson, 2003).

Information on the subsurface structure of the Vestmannaeyjar archipelago is limited. The island of Heimaey is the largest, and the only inhabited, island. It is also where volcanic activity has been most common and where the thickness of volcanic formations is considered to be greatest (Jakobsson, 1979; Mattsson and Hoskuldsson, 2003). Two deep boreholes have been drilled at Heimaey and cuttings from these holes reveal the stratigraphy to  $\sim 2 \text{ km}$  depth. The 1964 drillhole near the north coast of the island is 1550 m deep. It reveals that the Vestmannaeyjar volcanic formation, mostly hyaloclastite tuffs, reached only to 180 m depth; from 180 to 820 m depth, volcaniclastic basaltic marine sedimentary rocks are the dominant formation (Tomasson, 1967). The 2005 hole is 2276 m deep and located  $\sim 2.5 \text{ km}$  to the southeast of the 1964 hole. It gives very similar results (Gunnarsson et al., 2005). The volcaniclastic sedimentary rocks underlying the Vestmannaeyjar volcanic are most likely derived from south Iceland, originating as volcanic particles produced by eruptions on the mainland or through glacial or fluvial erosion. A schematic cross-section of the Vestmannaeyjar archipelago and its relation to mainland Iceland is presented in Fig. 2. It is based on the two drillholes on the island of Heimaey and geophysical surveys in the ocean between Heimaey and the Icelandic mainland (Thors and Helgason, 1988; Gunnarsson et al., 2005). To the south of Heimaey, little data exists on the thickness of the volcaniclastic sedimentary rocks or the possible existence (or absence) of shallow intrusive bodies.

## 4. The 1963–1967 Surtsey eruption

Volcanic activity was observed near the southern tip of the Vestmannaeyjar archipelago on 14 November 1963, where pre-eruption ocean depth was about 130 m (Thorarinsson et al., 1964). This was the beginning of the Surtsey eruption. Seismic tremor records, however, indicate that the submarine eruption started on 12 November 1963 and reached the surface to become subaerial about 40 h later (Sayyadi et al., 2021, 2022) in the early morning of 14 November (Thorarinsson et al., 1964). Eruptive activity continued until June 1967 (Thorarinsson, 1968b). Over this 3.5-year-long period, a volcanic island, Surtsey, and its satellite edifices (Surtla, the ephemeral islands of Syrtlingur, and Jolnir) were created (Fig. 1). The main phases of the 3.5-year-long eruption were:

Surtur (initially named Surtur I), November 1963 to January 1964. The explosive, subaerial eruption was preceded by  $\sim 40 \text{ h}$  of submarine eruption (Sayyadi et al., 2021).

Surtla, explosive submarine eruption, late December 1963 to early January 1964.

Syrtlingur (initially named Surtur II), explosive subaerial eruption, February to April 1964; effusive eruption, April 1964 to May 1965. Syrtlingur, initially submarine, progressing to subaerial explosive eruption forming an island with a tuff cone; May to October 1965. Jolnir, initially submarine, progressing to subaerial explosive eruption forming an island with a tuff cone, December 1965 to August 1966.

Surtur (Surtur I), effusive: August 19, 1966 – June 5, 1967.

The subaerial parts of Syrtlingur and Jolnir were washed away by wave action a few weeks after the end of the activity. The term Surtsey eruptive complex will be used hereafter to include all of these features. The island of Surtsey attained a surface area of  $2.67 \text{ km}^2$  at the end of the eruption period in June 1967. Erosion occurred rapidly in the years following the eruption, although the rate has declined over time; by 2019, about 45% of the lava fields had eroded away but only about 16% of the tuff cones (Jakobsson et al., 2000; Oskarsson et al., 2020). The outlines of the island of Surtsey in 1965, 1975, and 2016, are shown in Fig. 1c.

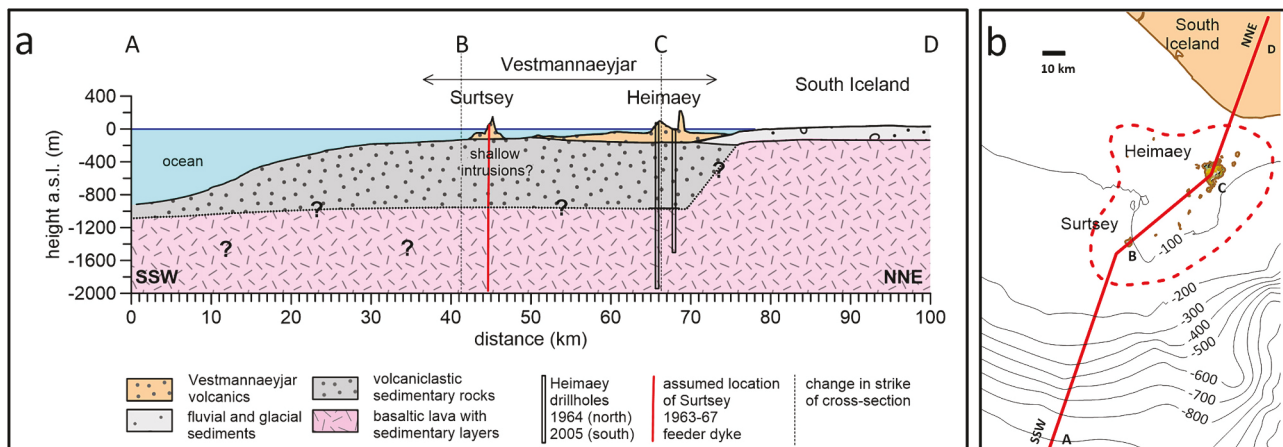


**Fig. 2.** a) A schematic cross-section of the Vestmannaeyjar archipelago and its connection to mainland Iceland, based on drillholes in Heimaey, limited seismic surveys, and other data (Tómasson, 1967; Thors and Helgason, 1988; Gunnarsson et al., 2005). The thickness of volcaniclastic sedimentary rocks south of Heimaey is uncertain. b) Location of cross-section (bathymetry data from the Icelandic Coast Guard Hydrographic Survey).

## 5. Survey setup

The aeromagnetic survey was conducted on 30 October 2021, using MagArrow Geometrics, a laser-pumped, cesium vapor magnetometer (photo of the instrument in Appendix C), designed originally for drone

surveys (Geometrics, 2019). It was set up with the MagArrow fastened by two rigid aluminum poles to the bottom of a Partenavia Observer II aircraft, allowing the MagArrow to be lowered 1.2 m below the aircraft while surveying. The survey area (Fig. 3) is 6 by 10 km in size ( $60 \text{ km}^2$ ) and was covered in 6 h. The area includes Surtsey and its surroundings,

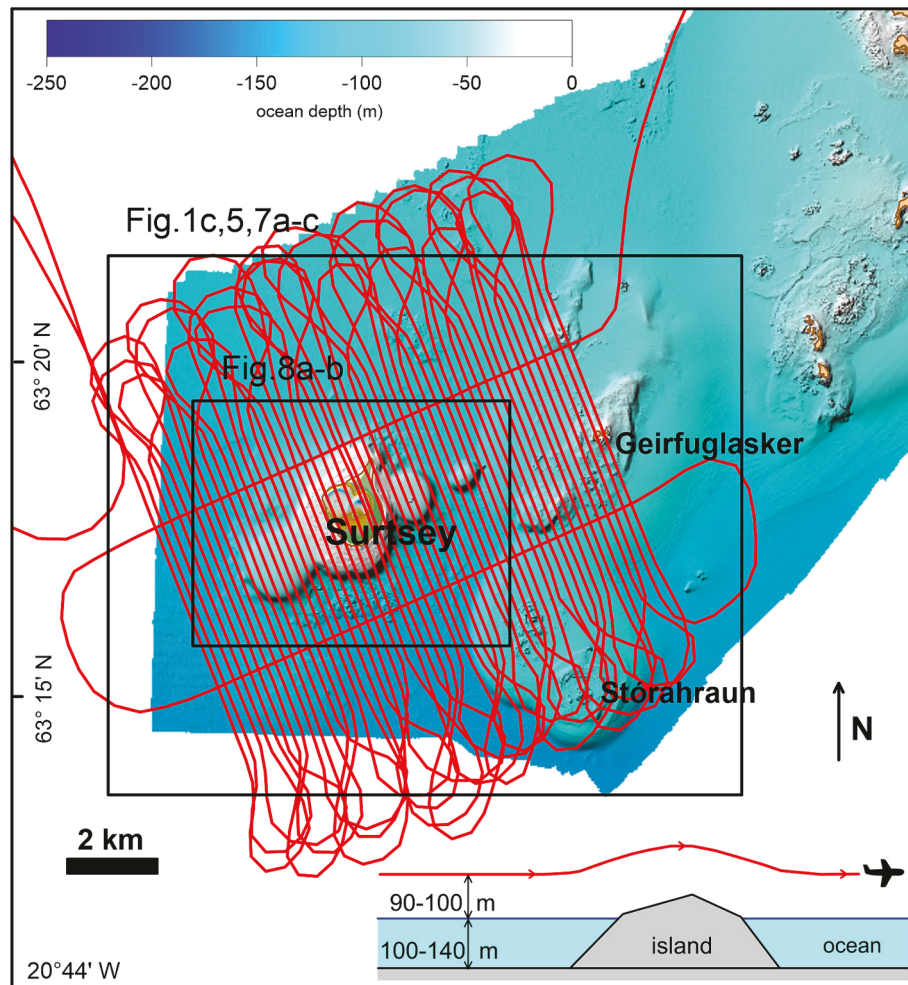


**Fig. 3.** The October 2021 aeromagnetic survey. The rectangles indicate the areas shown in Figs. 1c, 5, 7a-c and 8a-b. The schematic sketch at the bottom shows the aircraft's altitude and clearance.

the island of Geirfuglasker, and the area to the east and northeast of Surtsey with undulations in the seabed that are considered traces of past eruptions (Fig. 1). Flight lines were flown either NNW or SSE and had a spacing of 200 m, similar to the mean depth from the aircraft to the seafloor in the area. Away from the island of Surtsey, the flightline elevation was approximately 90 m (~300 ft) above sea level. This does not apply to the lines crossing Surtsey which had a clearance of 100–200 m over the island while approaching 90 m a.s.l. at the northern and southern ends of the survey lines. Two tie-lines were flown at right angles (ENE and WSW) to the main survey line directions.

## 6. Data processing and the magnetic map

The MagArrow has a sampling rate of 1000 Hz. The speed of the aircraft was close to 50 m/s, so the distance between individual measurements was 5 cm. The data processing involved the following steps:

- (1) In order to make the data more convenient for processing with no loss of resolution, it was resampled with a moving average to a frequency of 20 Hz, giving a point spacing of 2.5 m.
- (2) A low pass filter with a frequency of 0.1 Hz was applied. This removed low amplitude high-frequency noise associated with the aircraft from the data while preserving anomalies arising from sources at >200 m below it.
- (3) Temporal variations were removed using the record from the Leirvogur Magnetic Observatory, 110 km NE of Surtsey (<http://cygnus.rhi.hi.is/~halo/leirvogur.html>). Apart from a diurnal variation (a few nT), the geomagnetic field was quiet at the time of the survey.
- (4) A static shift in the magnetic field strength of about 80 nT was observed, depending on flight direction (NNW versus SSE). This effect was removed.

The corrected data were used to create a magnetic map with 100 m grid spacing, using kriging (Golden Software, 2021). The final residual magnetic map, after removal of the IGRF12 reference field is shown in Fig. 4.

### 6.1. Magnetic properties

The Surtsey volcanic complex is composed of diverse deposits with basaltic compositions (e.g., Jakobsson, 1979). These include (1) lapilli tephra and lapilli tuff, including hyaloclastite, (2) subaerial lava, (3) submarine pillow lava, (4) submarine foreset (lava) breccias, the submarine components of lava deltas, (5) minor intrusions (dykes, sills, peperites) and (6) seafloor volcaniclastic sedimentary rock (Jakobsson and Moore, 1982; McPhie et al., 2020).

The magnetic properties of these deposits show highly contrasting values. Very young surficial deposits composed of products of magma fragmentation (lithified tephra, and mostly lapilli tuff composed mainly of originally glassy pyroclasts) commonly have very low net magnetization: 0–1 A m<sup>-1</sup> (Kristjansson, 1970). Magnetization was also measured in samples from the 2017 drill cores (Jackson et al., 2019, Table S2). These are 32 basaltic lapilli tuff reference samples and one basaltic intrusion, with sample locations spanning nearly 290 vertical meters of the Surtur deposits. These include samples from the subaerial tuff cone, and submarine deposits and extend to ~100 m depth into an explosively excavated subseafloor diatreme (Jackson et al., 2019, Table S2). The mean NRM value obtained for the lapilli tuff edifice above the seafloor was 0.8 A m<sup>-1</sup> while a mean value of 1.7 A m<sup>-1</sup> was obtained for compact lapilli tuff in the diatreme deposits; variations in the measured values derive from variations in the material and mechanical characteristics of the deposits (Jackson et al., 2024).

The basaltic volcaniclastic marine sedimentary rocks underlying the Vestmannaeyjar Archipelago, including the Surtsey region (Fig. 2),

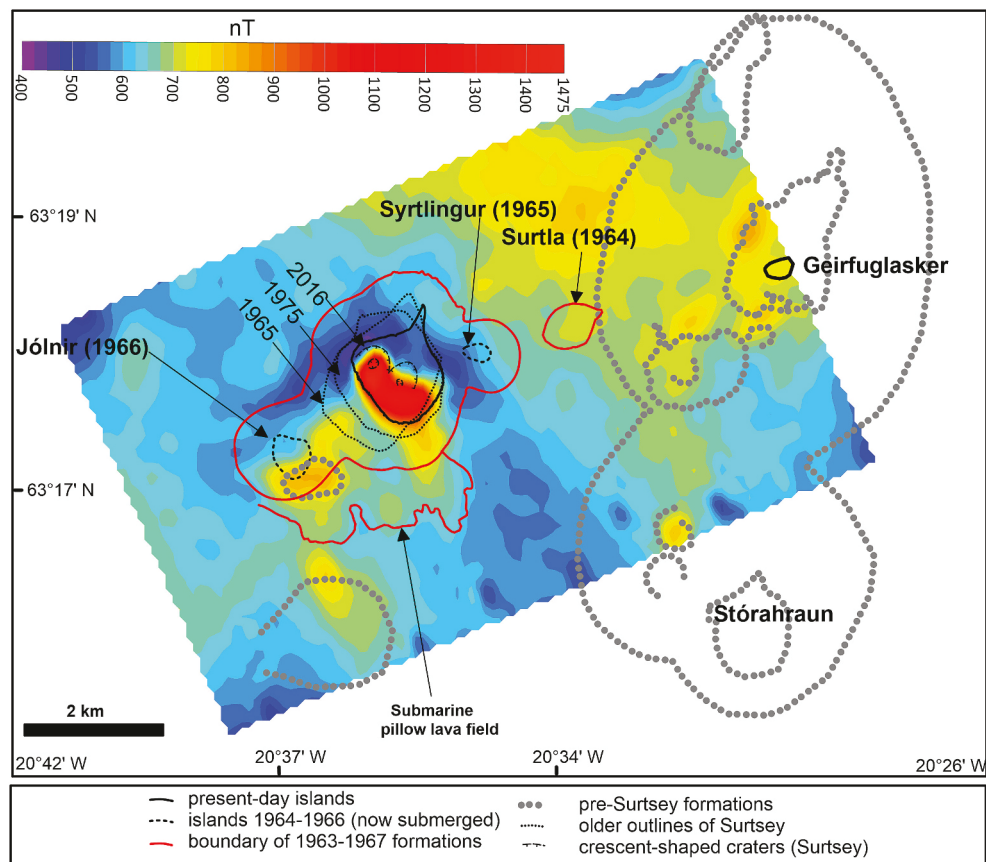


Fig. 4. A residual field magnetic map from the 2021 survey after subtraction of 51,926 nT; a value derived from IGRF12.

should have little net magnetization and are not expected to be the source of magnetic anomalies, forming a continuous extensive layer over the whole area (Thors and Helgason, 1988). In contrast, recently formed and presumably unaltered coherent basaltic rock, such as the subaerial lavas, pillow lavas, and intrusions are expected to have quite high magnetization (e.g., Kristjansson, 1982; Gudmundsson and Milsom, 1997; Kristjánsson, 2013). The sources of these magnetic anomalies are considered to be lava flows, pillow lavas, and intrusive rocks. In contrast, the submarine foreset breccias, formed by the seaward advance of the subaerial lava flows, are expected to be mostly composed of glassy and non- or weakly magnetized material.

The lava field that formed during subaerial effusive activity at Surtsey in 1964–1965 (Surtungur) and 1966–1967 (Surtur) is in most places 30–100 m thick (Thorarinsson, 1968a). The magnetization of these lavas was studied using 39 samples collected in 2018 (Appendix A). The remanent magnetization of these samples ranges from 2.2 to 29.6 A m<sup>-1</sup>, with a mean of 11.8 A m<sup>-1</sup> and a standard deviation of 7.3 A m<sup>-1</sup> (Fig. 5). The average susceptibility is 0.02, resulting in induced magnetization of about 0.8 A m<sup>-1</sup>. Thus, the remanent magnetization dominates, with the Königsberger ratio in most cases well above 10 (Fig. 5a). The magnetization of the dyke cored at 287 m vertical depth under Surtur crater is 19.5 A m<sup>-1</sup> (Jackson et al., 2019, Table S2; Weisenberger et al., 2022). Overall, these measurements confirm relatively strong magnetization of Surtsey basaltic lavas and intrusions, yet the large range does not support a single average value.

## 7. Results

### 7.1. Correlation between geological features and magnetic anomalies

The magnetic map in Fig. 4 shows several anomalies that appear to be associated with known geological features, while others do not have an obvious connection. By far the most prominent magnetic anomaly is located over the southern part of the island of Surtsey; it closely correlates with the subaerial lava shield. Other features constructed during the eruption also appear to have a spatial correlation with magnetic anomalies. These are the now submerged edifices of Jónir (1966) and

Surtla (1963–1964). A low-amplitude magnetic anomaly high is correlated with a suspected pillow lava field on the seafloor extending 0.5–1.0 km from the southern coastline of Surtsey (Sigtryggsson and Sigurdsson, 1966; Jakobsson et al., 2009).

The location of the magnetic high (~200 nT) that correlates with the southeastern edge of the submarine remnants of Jónir does not fit with the location of the vent that built up the temporary island (Fig. 5, black dashed line). However, it does fit with the location of a topographic knob (Fig. 5, gray dotted line) that appears on bathymetric maps made in 1964, prior to the Jónir eruption (Jakobsson et al., 2009), and on a seismic reflection profile surveyed in 1980 (Thors and Jakobsson, 1982). Thus, the magnetic high seems to correlate with a pre-existing structure. Furthermore, no magnetic anomaly is associated with the submerged remnant of the former island of Syrtlingur (1965). There is, however, a weak anomaly (~45 nT) on the three survey lines that cross the submarine remnant of Surtla. This anomaly was previously detected by a single boat traverse with a magnetometer in 1965, after the 1963–1964 Surtla eruption (Sigurgeirsson, 1966).

The magnetic anomalies that occur to the south and east of Surtsey are apparently associated with pre-Surtsey structures: Geirfuglasker and the northern part of the Stórahraun (Figs. 1c, 5). This includes a sharp anomaly over the northernmost of the craters associated with Stórahraun and three similarly sharp anomalies (amplitudes of 75–150 nT) to the north, southwest, and south of Geirfuglasker. The sharpness and spatial confinement indicate very shallow magnetic sources. These may be related to remnants of subaerial lavas formed during the last glaciation when the sea level was lower than today (e.g., Thors and Helgason, 1988). Broader magnetic anomalies occur in the northeastern part of the surveyed area. The source of these anomalies may be older – pillow lavas or other coherent basalt – structures not related to the formation of Surtsey.

### 7.2. Magnetic map analysis, depth to sources

Fig. 4 shows that the 60 km<sup>2</sup> area surveyed has several magnetic anomalies, including the Surtsey 1963–1967 eruption complex. The strength of these anomalies varies, but they have amplitudes that are

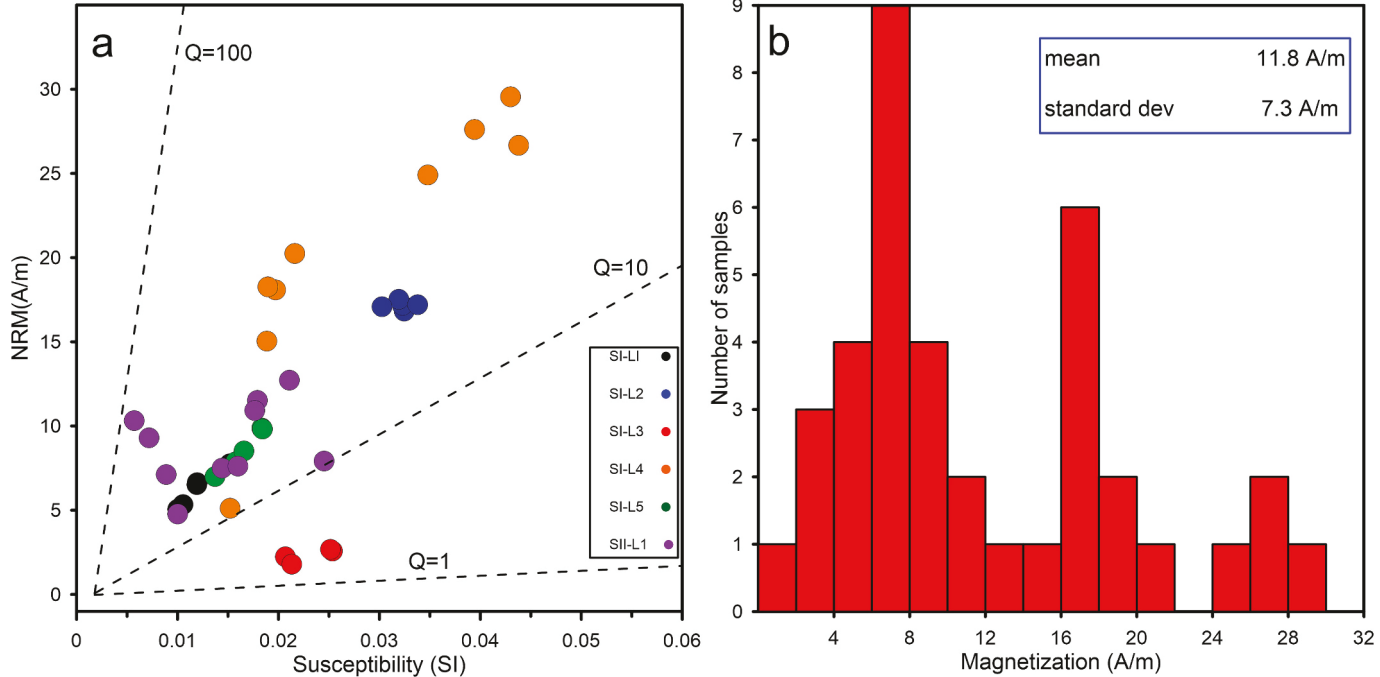


Fig. 5. Magnetic properties of Surtsey basaltic lava, see details in Appendix A. a) The Königsberger ratio (Q) and b) distribution of magnetization in samples of lava from Surtsey.

much lower than the ones produced by the lava flow field on the island of Surtsey. These magnetic anomalies have mostly short wavelengths ( $<1$  km), suggesting relatively shallow sources. To explore the depth of the sources we performed a 2D spectral analysis and Euler deconvolution. The magnetic field has a declination  $75^\circ$  at this location and is dominated by the vertical component. However, to avoid bias, before applying the spectral analysis and Euler deconvolution to the data, it was reduced to the pole (Appendix B). The reference surface of the analysis outside Surtsey is sea level; thus, a calculated depth of 100–150 m corresponds to a source at or very close to the seafloor.

The surface of the Surtsey lava field lies at 20–100 m above sea level. Over the island, the aircraft altitude was increased to 250–300 m a.s.l. (Fig. 3), resulting in a spacing of  $\sim 200$  m between the aircraft and the magnetic source over Surtsey. Thus, the lava should correspond to a reference depth of  $\sim 100$  m in the Euler and spectral analysis.

### 7.3. Spectral analysis

A radially averaged 2D power spectrum (Spector and Grant, 1970) for the survey area, using a reduced-to-pole map (Appendix B), is shown in Fig. 6, obtained by applying the Geosoft software (Geosoft, 2015). Since the spectrum is radially averaged, it is independent of any linear or other spatial trends that may be present in the data. The decay of the spectrum function, shown by the slope of Fig. 6a, within a comparable wavenumber range, indicates the depth of the causative bodies but does not provide information on the location of individual bodies.

The highest wavenumber signal shown in Fig. 6 ( $>4$  km $^{-1}$ ) represents noise and does not contain information on magnetized bodies. The first part of the spectrum graph (wavenumber  $<1$  km $^{-1}$ ) refers to the deepest bodies that may be present. Wavenumbers in the range 1–4 km $^{-1}$  dominate the middle to low frequency region. The average depth to the shallower sources is calculated from the slope for this wavenumber range (Fig. 6a) (Reid et al., 1990).

Fig. 6b shows the results from the spectral analysis on depth to sources for the area surveyed. The results indicate that most anomalies arise from shallow bodies, at depths of 100–400 m below sea level. This implies that the island of Surtsey and the uppermost 300 m of the seafloor is the source region, with the shallowest sources being the most common.

### 7.4. Euler deconvolution

To further analyze the depths of the magnetic sources and how they vary over the magnetic survey area, we apply Euler deconvolution (Reid et al., 1990). It requires neither information on the magnetization direction of the field nor of the sources (Mushayandebu et al., 2001). Rather, it is utilizing how the shape and extent of the anomalies vary with the form of the causative bodies. Calculated values of depth depend on the type of body form chosen. Since the shape of the source bodies is usually poorly known, Euler deconvolution is applied using a range of different shapes of the causative bodies, with body form expressed through the structural index (SI). For dykes and sheets SI = 1, for vertical

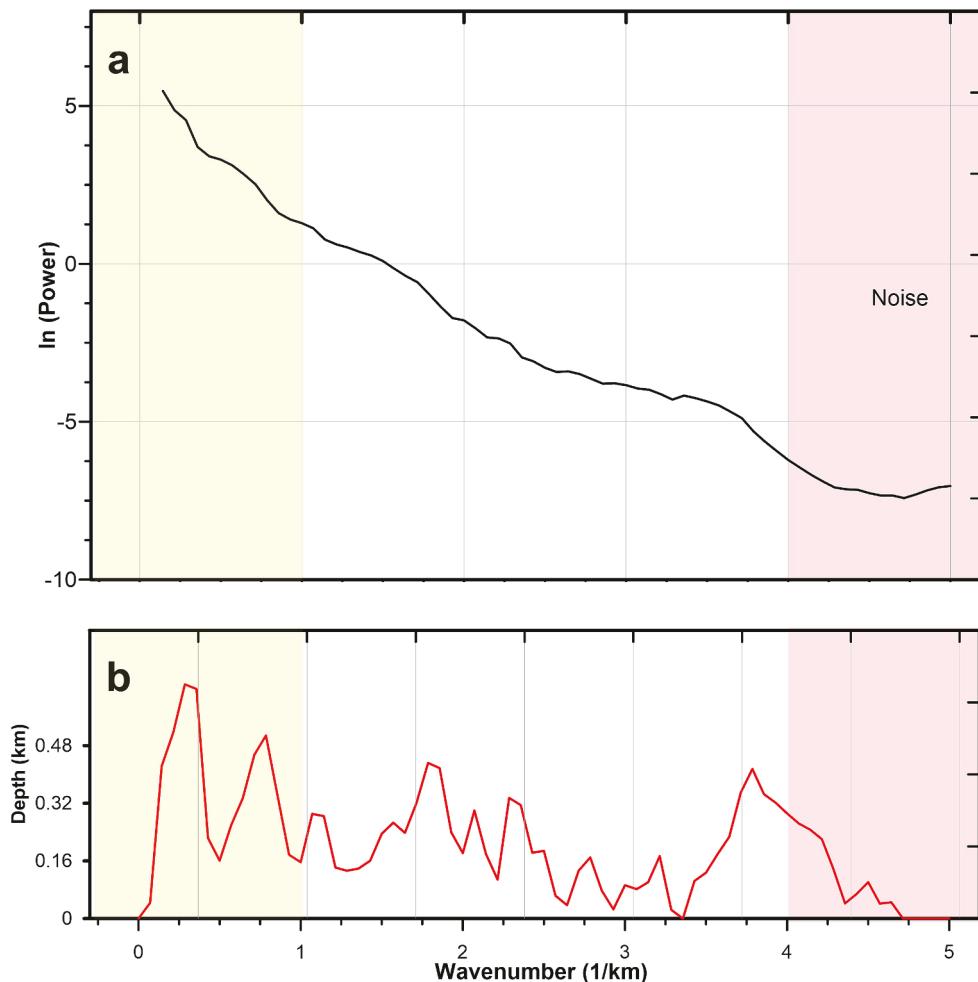


**Fig. 6.** Radially averaged power spectrum (a) and depth estimation (b) of anomalies for the area covered by the magnetic survey. The spectra are obtained using the Geosoft software (Geosoft, 2015) and indicate a dominant source depth in the uppermost 300 m of the seafloor.

pipes  $SI = 2$ , while bodies that are spatially small compared to the depth and therefore resembling dipoles, have  $SI = 3$  (Reid et al., 1990). The magnetized bodies would have mainly formed by the flow of magma through a dyke or a pipe-like conduit and, in reality, such pipes or vertical sheets should be associated with the bodies. However, such conduits are likely short, narrow dykes below the  $SI = 3$  bodies and are therefore considered to be minor sources of anomalies. We use the Geosoft software (Geosoft Inc., 2015) for the calculation of the 3D-Euler deconvolution for the magnetic grid (Fig. 4) and the three structural indices mentioned above ( $SI = 1$ ,  $2$ , and  $3$ ). The results are shown in Fig. 7.

Depth is relative to the ocean surface, as before. Fig. 7a suggests that  $SI = 1$  source shapes, as horizontally emplaced sills or vertically emplaced dykes, would occur at depths  $<130$  m. Thus, structural index 1 calls for unrealistically shallow sources for dykes, forcing  $>50\%$  of solutions to physically implausible depths above the seafloor (Fig. 7d). Fig. 7b suggests that  $SI = 2$  source shapes, such as pipe-like eruptive conduits, would occur over a large range of depths. However, about 25% of

the structures are forced above the seafloor. Fig. 7c suggests that  $SI = 3$  source shapes, as dipole-like spherical structures, would occur at depths at or below the seafloor. This analysis appears most realistic, with possible sources being submarine lavas or shallow intrusions. The results therefore indicate that  $SI$  in the range 2 to 3 is most plausible for the mapped area. Note, however, that the lava field on Surtsey with an approximate length of 1.5 km (NNW-SSE) and a width of 750 m (ENE-WSW) (Figs. 1b, 5), would be better represented by a sheet with  $SI = 1$ . This feature, located at 20–100 m above sea level is not well-represented by the Euler deconvolution analysis of  $SI = 1$ . It should also be noted that the overall results from the Euler deconvolution agree with the 2D spectrum (Fig. 6b), in that most sources appear to be located in the uppermost 200–300 m of the seafloor.

Comparison of the estimates for depth to the source using spectral analysis (Fig. 6) and Euler deconvolution (Fig. 7) for the magnetic grid map (Fig. 5) shows that the two methods provide essentially identical results: the principal sources for magnetic anomalies in the Surtsey region arise from shallow sources.

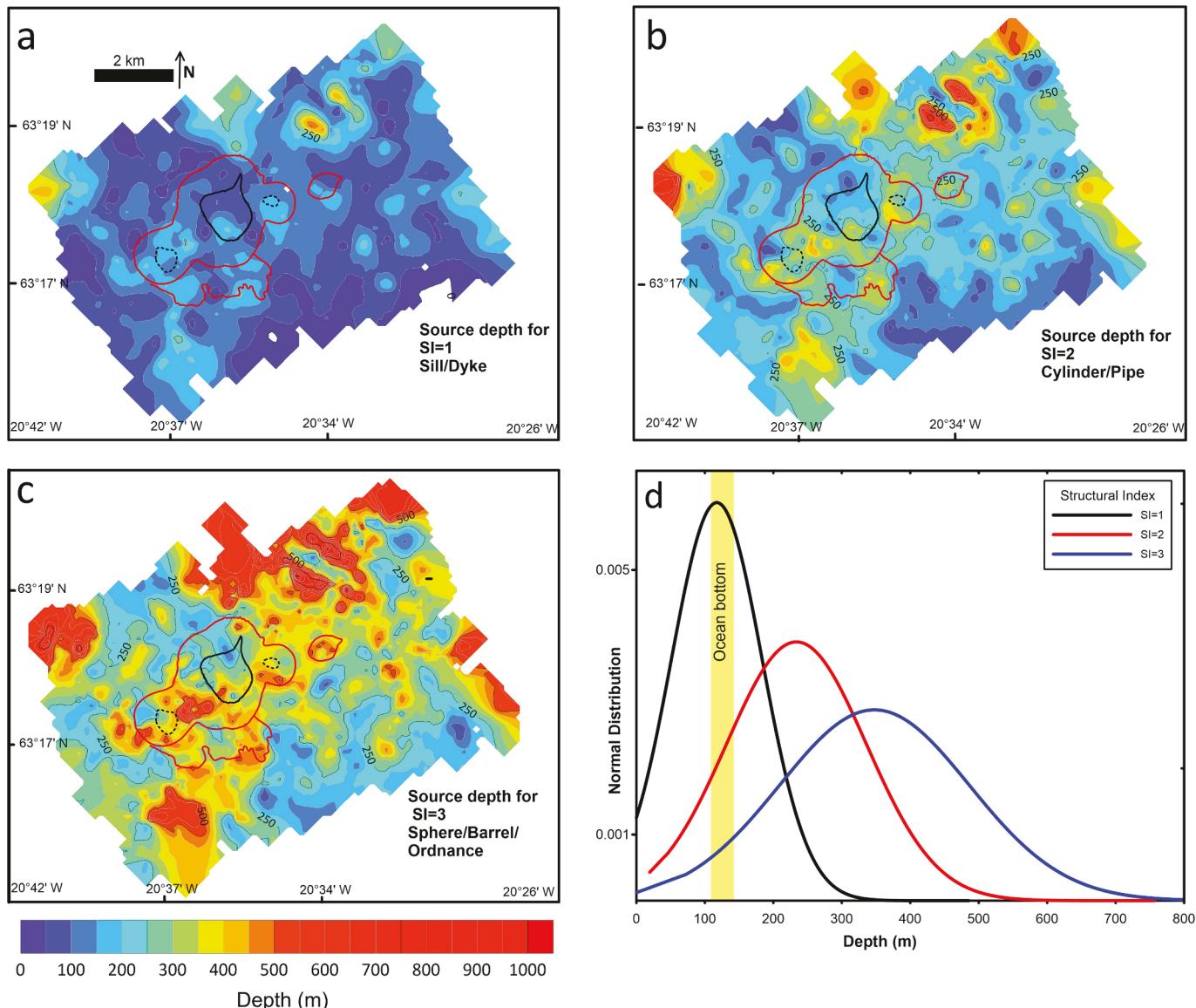


**Fig. 7.** Depth estimation relative to the ocean surface for causative bodies according to 3D-Euler deconvolution of the reduced to the pole magnetic map (Appendix B) for different structural indexes. The area shown is the same as in Figs. 1c and 5. (a) sheet (resembling sills or large dykes);  $SI = 1$ , (b) vertical pipe (resembling e.g., eruptive conduits);  $SI = 2$ , and (c) sphere (bodies of spatial extent small compared to their depth, e.g., knobs of pillow lava or intrusions);  $SI = 3$ . d) depth distribution of sources for each  $SI$ .

## 8. 3D forward magnetic modeling of Surtsey volcanic structures

### 8.1. Model construction and approach

For further analysis, we have constructed a 3D forward model that

considers the full spatial extent and geometry of the geological features of interest. The forward model takes a layered approach where geological bodies are defined by upper and lower surface grids. As visualized in Fig. 8, this layered stratification allows for a reasonably comprehensive and continuous analysis of the geometry of associated

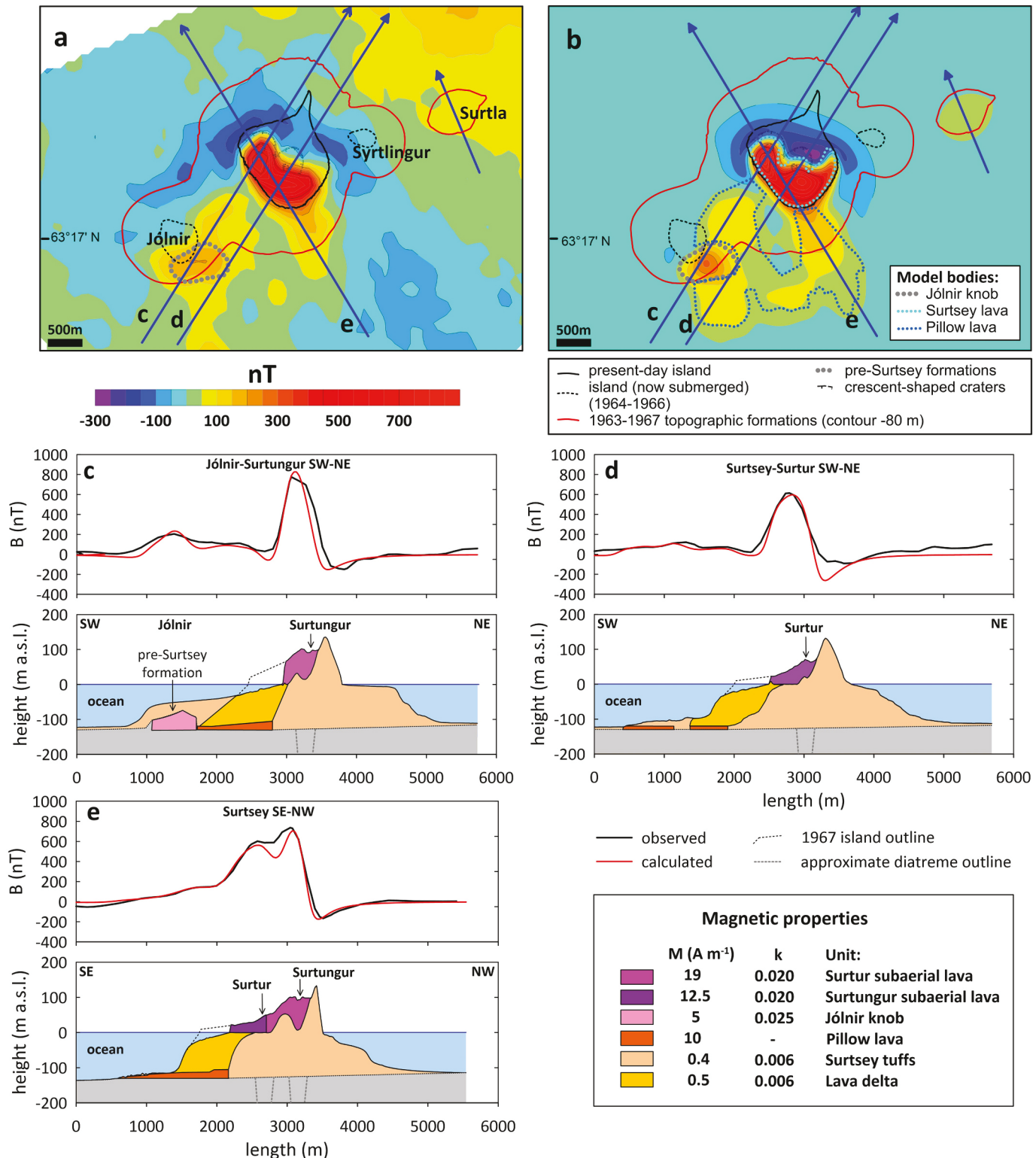


**Fig. 8.** 3D forward models of the Surtsey complex. a) Map of the observed residual field with 630 nT subtracted (see text). b) Model map of the survey area with outlines of the model bodies contributing significantly to the anomalies observed for the Surtsey subaerial lavas, Jólnir knob and pillow lava field (south side of the Surtsey). c) SW-NE cross-section over Jólnir and Surtungur, d) SW-NE cross-section over Surtur, e) SE-NW cross section for Surtur and Surtungur at Surtsey, including the modeled pillow lava sheet.

structures, essential for identifying as much as possible of the subsurface structure of the Surtsey volcanic complex. This is done with the 2022 version of Geosoft's GM-SYS 3D (Geosoft, 2022) modeling software, using the Parker (1972) algorithm. This software constructs models using multiple stacked surface grids, where each layer's, magnetic susceptibility ( $k$ ), and remanent magnetization ( $M$ ) are specified using the empirical data (Fig. 5) to delineate different geological features.

## 8.2. Geological bodies and magnetization parameters

The 3D model incorporates six principal geological bodies: (1) the edifice built in the explosive phreatomagmatic phase of 1963–1964, made of lapilli tephra and tuffs; (2) the Surtsey subaerial lava field formed in 1964–1967; (3) the submarine lava delta formed in 1964–1967; (4) the pillow lava field on the sea floor south of Surtsey, and the two bodies formed in eruptions outside the island of Surtsey that give rise to magnetic anomalies; (5) the Jolnir knob; and (6) Surtla. The magnetization values used for bodies (1) and (2) are derived from field samples (Fig. 4), while the values used for bodies (3), (4) and (5) are less well-constrained. However, values obtained for similar basaltic formations in Iceland are used to provide plausible constraints (e.g. Kristjansson, 1970; Kristjansson, 1982). Fig. 8a shows the magnetic map of the model area, where 630 nT have been subtracted from the residual map (Fig. 5) in order to remove the remaining residual mean field after subtraction of the IGRF. Fig. 8b shows the modeled field while Fig. 8c–e are cross-sections providing a comparison between the model and the measured field.

- (1) **The lapilli tephra and tuff:** The geometry of this body is well constrained by maps from 1964 (Thorarinsson, 1967c). It makes up the largest volume of the submarine volcanic edifice (Fig. 8). It is assigned the mean magnetization and susceptibility values obtained from lapilli tuff reference samples in the uppermost 100 m of the drillholes (equivalent to  $0.6 \text{ A m}^{-1}$ , see Appendix A) (Jackson et al., 2019).
- (2) **Surtsey lava:** The topography of the island in 2021 (at the time of the survey) and at the start of effusive activity in April 1964 (Thorarinsson, 1967c), provides strong constraints on the geometry of the lava flows erupted from Surtungur (April 1964–May 1965) and Surtur (August 1966–June 1967) (Fig. 8d and e). The magnetization and susceptibility are constrained by the outcrop sample analyses (Fig. 4, Appendix A). A better fit is obtained by assigning different magnetization values to the Surtungur and Surtur lavas; ( $12.5 \text{ A m}^{-1}$  for Surtungur,  $19 \text{ A m}^{-1}$  for Surtur); this difference is supported by the values obtained for the samples for each lava (Appendix A). These values fall within the range provided by the surface lava samples ( $12.6$ – $7.3 \text{ A m}^{-1}$ ) (Fig. 4; Appendix A).
- (3) **The lava delta:** Magnetization assigned to the lava delta is low, similar to that of the lapilli tuffs (equivalent to  $0.7 \text{ A m}^{-1}$ ). The submarine lava delta is inferred to consist of largely glassy deposits having only minor amounts of coherent magnetized rock (e.g., Watton et al., 2013); explaining the low magnetization assigned to it of  $0.7 \text{ A m}^{-1}$ .
- (4) **The Jolnir knob:** The seismic (Thors and Jakobsson, 1982) and bathymetry data (Vestensson, 2009) provide some constraints on the thickness and extent of the body. It is modeled as  $30$ – $40 \text{ m}$  thick. By using magnetization of  $5 \text{ A m}^{-1}$  and susceptibility of  $0.025$ , a reasonable fit is achieved. This body is graphically represented by the pronounced peak in the observed magnetic field data on the SW-NE profile (Fig. 8c).
- (5) **The pillow lava field:** The size and form of this body is poorly known in comparison with bodies 1–4. It is only constrained to the south of Surtsey and its extent or thickness under the island is unknown. The approach taken here is to use an initially  $10 \text{ m}$  thick layer between  $120$  and  $130 \text{ m}$  depth and allow it to extend

under the island approximately to the boundary between the lava delta and the margin of the lapilli tuff edifice (body 1). Here a value of  $10 \text{ A m}^{-1}$  is assumed, an approximate value for basaltic pillow lavas in Iceland (e.g. Kristjansson, 1970). The best fit is obtained by the gradual thickening of this layer towards the island.

The modeling suggests that the subaerial lava is the principal source for the  $\sim 700 \text{ nT}$  anomaly in the southern sector of Surtsey (Fig. 4). The modeling also conforms to the low magnetization lapilli tephra and tuff dominating the subaerial and submarine deposits of Surtsey, both for Surtur and Surtungur. This is consistent with drill cores acquired in 1979 and 2017 (Jakobsson and Moore, 1982; Jackson et al., 2019; McPhie et al., 2020), which reveal only small amounts of coherent basalt as dykes (or other intrusions) emplaced within the pyroclastic deposits. A substantial deposit of early pillow lava erupted on the seafloor at the initiation of activity at either the Surtur or Surtungur vent would be difficult to reconcile with the measured magnetic anomalies. If such a body existed at the seafloor,  $300$ – $400 \text{ m}$  below the survey flightline over the island (Fig. 8c–e), the depth and likely extent beyond the diatremes would give rise to a considerably broader anomaly than observed.

The model results are consistent with the anomaly south of the island of Surtsey (Fig. 4) being caused by a sheet of pillow lava, formed as magma was channeled down through the lava delta during the absence of visible surface lava flow for 10 weeks (end of April–July 9, 1964; Thorarinsson, 1966) and emplaced on the seafloor. As stated above, the extent and thickness of this body are poorly constrained compared to other formations. However, the results indicate that this pillow lava field may cover  $2.5$ – $3.0 \text{ km}^2$  and have a volume of  $25$ – $40 \text{ million m}^3$ .

The apparent absence of any magnetic anomaly that correlates with the main edifices of Syrtlingur, formed in 1965, and Jolnir, formed in 1966, suggests that these structures have very minor, almost zero magnetization. This indicates that both edifices are formed of basaltic tephra/tuffs, with dykes and/or other coherent basalt forming volumetrically insignificant components of the structures.

**Surtla:** Surtla was formed in a submarine eruption at the end of December 1963 and the first days of January 1964. A cross-section through the 3D model of the submarine Surtla structure (Fig. 8b) is shown in Fig. 9. There are two plausible scenarios for the observed anomaly: a primary dyke structure or an aggregation of crystalline and magnetized rocks within the edifice. The model utilizes magnetization and susceptibility values that offer an approximate fit to the observed anomalies, using values similar to the apparent magnetization of the weakly-consolidated tephra acquired by the 2017 drill cores at Surtur (Jackson et al., 2019). There is some discrepancy in the fit, however, and a dyke may also contribute to the anomaly. The existence of that dyke is supported by the presence of coherent basaltic boulders at the submarine ridge (Kokelaar, 1983; Jakobsson et al., 2009). If the bulk of the edifice of Surtla has very minor magnetization and susceptibility, similar to the remains of Syrtlingur and Jolnir, then a contribution from a dyke is indeed a plausible explanation. Moreover, the presence of peperites and/or dispersed small coherent crystalline intrusions as documented for subglacially formed edifices (e.g. Schopka et al., 2006) cannot be excluded, but these would only account for a minor part of the volume of Surtla. Moreover, the modest amplitude of the anomaly ( $\sim 45 \text{ nT}$ ) is not consistent with the presence of a substantial body of pillow lava at the base of Surtla. The modeling, therefore, suggests that Surtla could be a mound of basaltic tephra, with or without a narrow basaltic dyke that traverses the structure.

## 8.3. Model limitations

The fit obtained from the 3D forward models does not reproduce all the details seen in the magnetic map. Elaborate adjustments to the geometry or allowing for variable magnetization and susceptibility for individual bodies could be applied to improve the fit. However, this

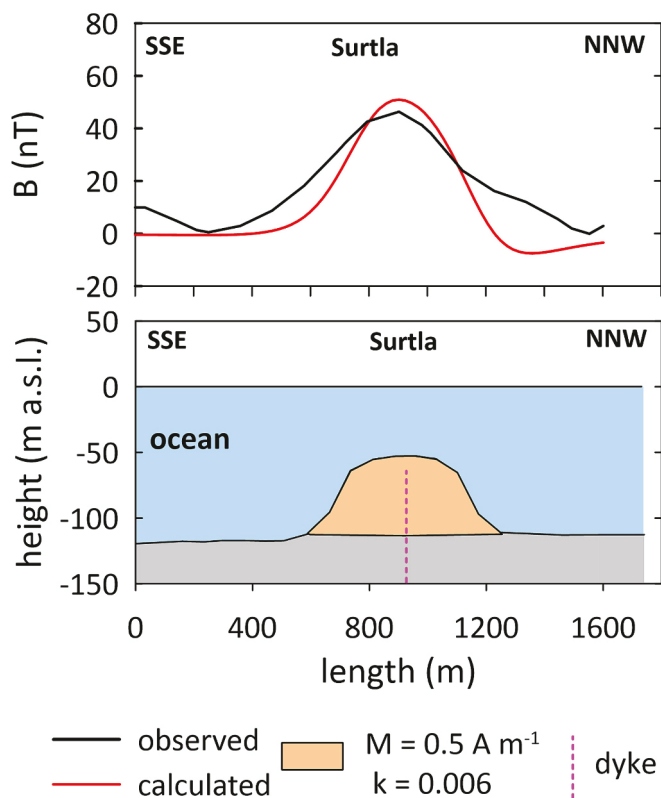


**Fig. 9.** SSE-NNW cross-section through Surtla, showing a profile of the observed field with a regional gradient removed, and the 3D modeled field (see Fig. 8a, b).

would not change the results in any significant way for the bodies modeled. For the profiles shown in Fig. 8d and e, the model has lows of 100–200 nT (over the tephra rim of Surtur in 8d and over the buried tephra rim between Surtur and Surtungur in 8c), much larger than the minor lows seen in the actual data. A possible explanation for this discrepancy is that the Surtur rim has some small and shallow dikes or intrusions formed during minor volcanic activity in December 1966 or January 1967, including the formation of a small lava flow on the north side of the island (Thorarinsson, 1968a, 1968b). The inclusion of such bodies could improve the fit at these locations but would not change the overall results.

#### 9. Comparison of the surveys in 2021 and 1965

A helicopter survey with a proton precession magnetometer was flown at 200 m elevation above sea level on 31 August 1965, covering Surtsey and extending 1–1.5 km beyond the 1965 shoreline (Sigurgeirsson, 1968). Importantly, this survey was performed after the eruption of Surtungur (1964–65) but before the formation of Jónlir and the effusive eruption of Surtur (Surtur I). In Fig. 10, the results of this survey (10b) are compared with the 2021 survey (10a). Data from Leirvogur Magnetic Observatory in Iceland compensates for the observed changes in total field strength between 1965 and the 2021 survey. An additional 130 nT was added to the 1965 survey map to remove a residual shift between the 2021 and 1965 maps away from the island of Surtsey. This discrepancy is probably due to the shifts applied to the data sets when directional effects are removed, as described in Section 5. Since the survey in 1965 was done at a 200-m height, an upward continuation filter (Blakely, 1995) has been applied to the magnetic grid map of 2021 (Fig. 5) lifting it by 100 m.

The map in Fig. 10c shows the difference between the field strength mapped in the 1965 and 2021 surveys. It reveals that large changes have

occurred in some locations. Firstly, the field strength has dropped by 400–450 nT in the area where erosion has removed the southwest sector of the island over the 54-year period between the surveys (Óskarsson et al., 2020). Secondly, the anomaly over the lava field has increased by 300–350 nT, in particular in the eastern sector where lava was emplaced during the Surtur effusive eruption of 1966–1967, post-dating the 1965 survey. Another contributing factor to the observed increase in anomaly strength in the western part of the lava field may be that the lava had not yet acquired full magnetization 1965. The flow was emplaced during the 1964–1965 Surtungur effusive activity and the 20–100 m thick lava stack (Thorarinsson, 1966) had not everywhere cooled through its Curie point.

Over the seafloor pillow lava field to the south-southeast of Surtsey, no apparent change appears between the 1965 and 2021 surveys (Fig. 8a, b). It seems that the pillows would have already formed and cooled, consistent with emplacement in spring 1964 (e.g., Jakobsson et al., 2009).

The anomaly associated with the topographic knob adjacent to the SE sector of Jónlir is visible in both the 1965 and 2021 magnetic maps. The knob also appears on the bathymetric map made in 1964 (Jakobsson et al., 2009; Vésteinsson, 2009). It therefore existed when the Jónlir eruption took place in 1966. A question arises as to whether this knob could represent a submarine lava mound formed in the first days of the Surtsey eruption in November 1963. The eruption is considered to have started on the ocean floor in the afternoon of November 12, based on seismic tremor (Sayyadi et al., 2021). Thermal anomalies were then detected 3–4 miles to the southwest of Surtsey on the morning of November 13, 1963, and in the vicinity of Surtsey on November 14 (Malmberg, 1965). Further measurements of sea surface temperatures were made in the vicinity of Surtsey on November 15 and 16, one and two days after the eruption became visible (Malmberg, 1965). The measurements were made along N-S and E-W lines, with the incipient island of Surtsey in the middle, and the closest observations occur 300 m from the emerging island. No heating was detected during these surveys. This suggests that no significant heat sources were present on the seafloor after Surtsey emerged on November 15, implying that the knob existed before the onset of the Surtsey eruption. Had a basaltic lava edifice of this size been present and only a few days old on 16 November, it would have been releasing significant heat to the water column, as, for example, was observed during the El Hierro eruption in the Canary Islands in 2011 (e.g., Rivera et al., 2013).

#### 10. Discussion

This study demonstrates the potential for the analysis of aeromagnetic survey data coupled with detailed bathymetry data to provide insights into past eruptive activity in shallow submarine settings. This applies, in particular, to volcanic structures formed within and/or on top of thick sedimentary sections that do not themselves produce magnetic anomalies. In such settings, the magnetized bodies would be submarine lavas, including pillows, buried bodies of subaerially erupted lava formed during episodes of lower sea level, and magmatic intrusions of significant crystallinity and thickness.

A limitation, however, is that only larger-scale features and their overall bulk properties can be accurately deciphered through aeromagnetic surveying and modeling. During the 2021 survey, for example, the minimum clearance between the aircraft and magnetometer and sources was ~200 m, implying that magnetized bodies must have a sufficiently large spatial extent and/or magnetization in order to produce significant, detectable anomalies.

The modeling (Figs. 8 and 9) suggests that the pyroclastic products of the 1963–1967 Surtsey eruption are mainly weakly- or non-magnetic below sea level. No significant anomalies seem to arise from the tephra and lapilli tuff deposits that were produced by explosive eruptive activity at Surtsey, Syrtlingur, and Jónlir. An exception to this is a pillow lava flow field visible in bathymetry, which is interpreted to have been

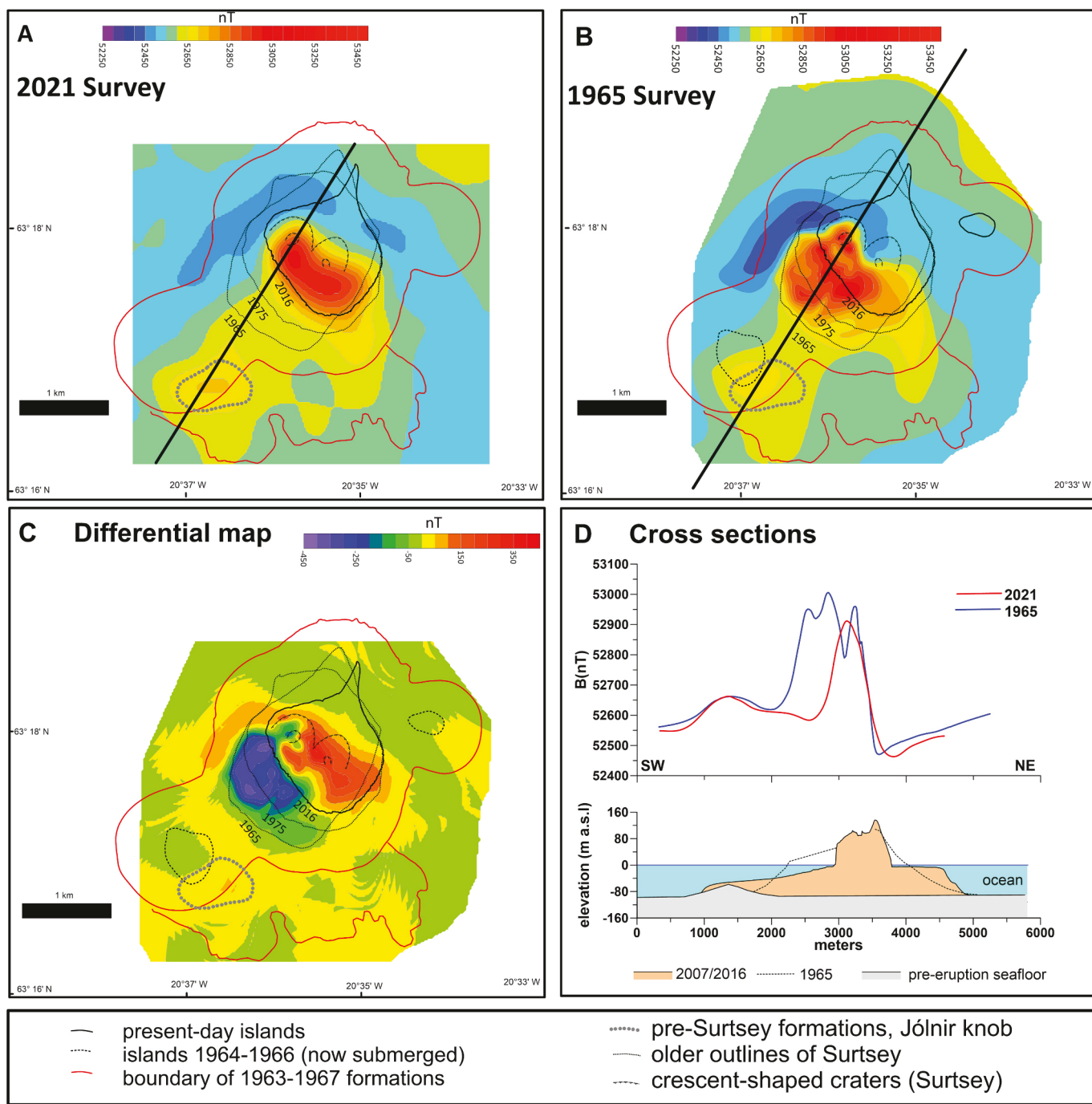


**Fig. 10.** a) The 2021 map of the total field continued upwards to 200 m above sea level. b) The magnetic map from the 1965 survey, with 1095 nT added to remove a static shift, mostly caused by changes in average field strength in Iceland between the dates of the two surveys (see text). c) Differential map showing the change in magnetic anomaly map between 1965 and 2021. d) SW-NE cross section (see locations in a and b) showing the change in magnetic anomalies between 1965 and 2021.

fed by magma channeled through the lava delta that extends south and southeast from the island of Surtsey (Figs. 5 and 8). Above sea level, the lava flows are highly magnetic and produce the strongest source of anomalies (Figs. 4 and 8).

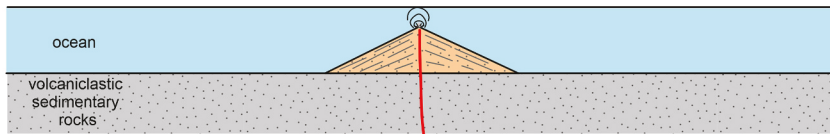
The coupled modeling of aeromagnetic data with bathymetry data suggests four different styles of eruption and emplacement of volcanic deposits within the Surtsey 1963–1967 complex. These phases are summarized in the schematic sections shown in Fig. 11: mildly explosive submarine activity (Fig. 11a), Surtseyan explosive activity (Fig. 11b), subaerial effusive eruption building a lava delta (Fig. 11c), and submarine effusive eruption forming an ocean-floor pillow lava field with

lava transported down a lava delta (Fig. 11d). This characterization largely agrees with previous work (see e.g. Jakobsson et al., 2009; Jackson et al., 2019), but also provides new constraints on the contributions and importance of the different phases.

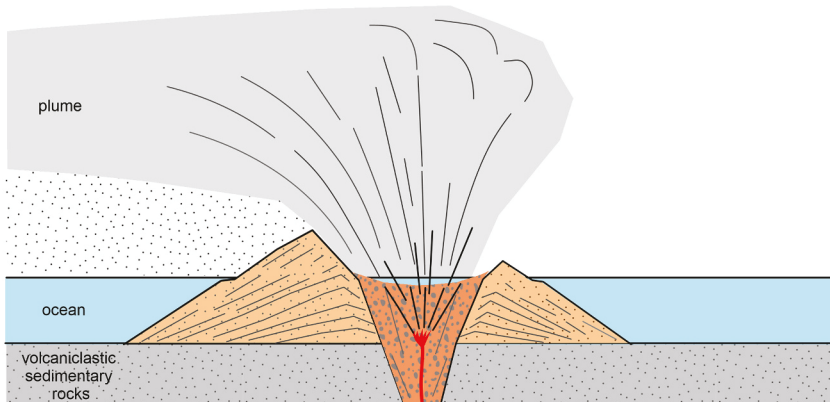
#### 10.1. Submarine to emergent explosive Surtseyan activity

The two stages of explosive activity are presented in Fig. 11a and b. Surtseyan explosive activity (Fig. 11b) was dominant from November 1963 to April 1964 and during the formation of the ephemeral islands of Syrtlingur (1965) and Jólnir (1966), building tuff cones and causing

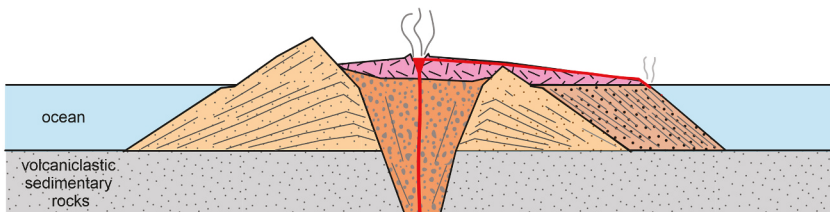
### A Submarine mildly explosive eruption: Surtla December 1963-January 1964



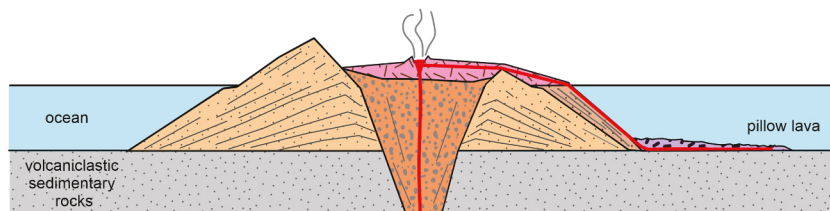
### B Surtseyan explosive eruption: Surtur 1963-64, Surtungur 1964-65, Syrtlingur 1965, Jólnir 1966



### C Effusive eruption Surtsey - formation of lava delta 1964-65 and 1966-67



### D Surtsey, pillow lava field formation - May-June 1964



#### very weak magnetization (0-2 A/m)

- [Grey box] oceanic tuffaceous sediments
- [Orange box] tuffs/tephra from explosive phases
- [Red box] diatreme/explosive crater fill
- [Dotted box] foreset breccia/lava delta

#### strong magnetization (~10-20 A/m)

- [Pink box] subaerially formed lava
- [Red box] pillow lava
- [Red line] dyke / lava path

**Fig. 11.** Schematic cartoons of four types of activity identified in the 1963–1967 Surtsey eruption, consistent with the magnetic survey results. a) Submarine magma fragmentation and the formation of a submarine cone. In the case of Surtla, activity terminated before the onset of more powerful Surtseyan explosive activity. b) Surtseyan activity with magma-water interaction. c) Subaerial effusive activity and the formation of lava flows and a lava delta. d) Formation of a submarine pillow lava field through channelized flow of magma from the subaerial vent, later partly buried by the advancing lava delta formed in 1964–1967.

tephra fallout of varying intensity. In comparison, the activity observed at Surtla was of much less intensity (Fig. 11a), as discussed further in section 10.2. Subaqueous explosive activity, forming the volcanic glass fragments that are the principal component of the submarine parts of the edifices of Surtur, Surtungur, Syrtlingur, and Jólnir, is expected to have

been the dominant style of the early submarine activity at all vents, progressing to Surtseyan style activity (Fig. 11b).

### 10.2. Mild explosive submarine activity, formation of Surtla

Differences exist between the magnetic anomalies of Surtla and those of Jolnir and Syrtlingur. The ephemeral islands of Syrtlingur and Jolnir were produced in explosive eruptions that added subaerial pyroclastic deposits to their apparently pyroclastic, very weakly magnetic, submarine deposits (Thorarinsson et al., 1964). Styles of the eruption from these islands were similar to those observed at the Surtur and Surtungur vents on the island of Surtsey (Thorarinsson, 1965, 1966, 1967c; Thorarinsson, 1968a, 1968b), which provides the only remaining record of subaerial deposits. Tabular feeder dykes for lava flows traverse lapilli tuff deposits on the surface of Surtsey. The 1979 and 2017 drill cores through the Surtur deposits encountered occasional intervals of coherent basalt, mainly 1 m in width, which have quenched margins and traverse the subaerial and submarine pyroclastic deposits (Jakobsson and Moore, 1982; McPhie et al., 2020; Oskarsson et al., 2020).

The feeder dykes for individual vents may have considerably greater total width. The 2017 angled SE-03 drillhole intersected the apparent subseafloor feeder of the Surtur effusive eruption of 1966–1967, a composite dyke that intruded the deep lapilli tuff section of the subseafloor eruptive conduit (Jackson et al., 2019; Weisenberger et al., 2019, 2022). The angled drill core traversed about 10 m of coherent basalt, from 342.4 to 352.0 m measured depth (McPhie et al., 2020). The horizontal trend of the drillhole has an angle of  $\sim 75^\circ$  from the trend of the volcanic fissure observed at the start of the activity (Thorarinsson, 1967b; Weisenberger et al., 2022). If the dyke has the same trend at depth, this indicates a total thickness of 5–6 m, formed during the 10 months of effusive activity. Important constraints on the volumetric contribution of the minor intrusions, feeders and other dykes, come from the 1979 and 2017 drill cores. Overall, intrusive crystalline rocks (dykes) constitute 19 m out of 727 m total in holes SE-01, SE-02B, and SE-03 (Jakobsson and Moore, 1982; Jackson et al., 2019; Weisenberger et al., 2019; McPhie et al., 2020), or 2.6 vol%. Using a magnetization of  $10\text{--}20\text{ A m}^{-1}$  would result in a volumetric average of  $0.3\text{--}0.6\text{ A m}^{-1}$ .

The edifice of Surtla, formed over 10 days in December 1963–January 1964, never grew above sea level to form an island. The observed phreatomagmatic activity at Surtla thus never reached the intensity of the explosions at Surtsey, Syrtlingur, and Jolnir. At Surtla, jets of steam and tephra only occasionally rose above the ocean surface, to a maximum height of 50 m on 29 December 1964, when activity was at its peak (Thorarinsson et al., 1964). The relatively mild subaqueous activity (Fig. 11a) may be the reason why a substantial crater with visible rims did not form at Surtla. Instead, the eruption left a steep-sided mound that may have preserved a large part of the dyke feeding the eruption. A scuba expedition in 1981 identified sparse blocks of vesicular basalt on this mound, which were interpreted as fragments of rare lava flow-units, possibly pillows or pahoehoe lava that were mixed with pyroclastic deposits (Kokelaar and Durant, 1983).

This survey can neither resolve the relative contributions of a dyke and/or peperites within the edifice nor prove the existence of one or the other. One possibility is that the anomaly is principally caused by a single dyke about 2 m thick. Alternatively, the sheetlike magnetic body at Surtla could represent a meters-wide fissure that was backfilled and mingled with enclosing pyroclastic debris during weakly explosive activity. Such a feature could share some characteristics with other fissure-filling deposits where erosion has removed weak country rock enclosing the upper few hundred meters of fissures linked with subaerial eruptions (e.g., Lefebvre et al., 2012; Re et al., 2016). No submarine equivalent is known, though spatter deposits formed during a submarine fissure eruption at Miyakejima in 2000 (Kaneko et al., 2005).

### 10.3. Subaerial and submarine effusive styles of activity

Two types of effusive activity are identified (Fig. 11c, d). Firstly, there are subaerial lava flows, partly built on lava deltas. Secondly, a submarine effusive eruption forming pillow lava on the seafloor appears

to have occurred in May–July 1964 (Jakobsson et al., 2009), sourced from the subaerial vent through channelized flow of lava. Conditions for this type of activity may have developed after the initial emplacement of subaerial lava and the establishment of a lava delta, and while lava flow rates were sufficiently high to maintain a stable channel down the lava delta.

### 10.4. Implications for assessment of submarine volcanic activity

The results presented here, based on the combined analysis of bathymetry data and aeromagnetic anomalies, have the potential to assist in assessing long-term volcanic production rates at distributed volcanic fields in shallow ocean settings, similar to the Vestmannaeyjar archipelago. Although the research does not directly address forecasting of long-term volcanic hazards, the results provide useful information for assessments of such hazards. This may include studies to assess the characteristics of volcanic deposits buried by seafloor sediments or intruded into the host sedimentary rock succession, as well as those of younger volcanic deposits. Moreover, insights into the geological and structural foundations of these volcanic fields enhance predictions of the pathways and potential impacts of future eruptions in similar shallow oceanic environments. These insights will assist in identifying areas at risk, understanding potential eruption dynamics, and informing mitigation strategies in oceanic and coastal settings vulnerable to Surtseyan volcanic activity.

## 11. Conclusions

Depth estimates obtained by 2D spectral analysis and Euler deconvolution indicate that, with the exception of the Surtsey subaerial lava field, all significant sources of magnetic anomalies are located on the seafloor or within the uppermost 200–300 m of the seafloor sedimentary rock succession.

By far the strongest anomaly is associated with the subaerial lava field on the island of Surtsey. The  $\sim 700\text{ nT}$  anomaly is best explained by  $12.5\text{--}19\text{ A m}^{-1}$  magnetization of the subaerial lava flow field, which formed in two episodes during 1964–1967.

The magnetic data are not consistent with the presence of significant volumes of highly magnetic rocks at or above the seafloor underneath the vent areas of Surtsey, supporting previous results and inferences that only very minor or no mounds of pillow lava were formed in the initial phases of the eruption.

A subtle magnetic high, observed to the south of Surtsey, can be explained by a  $\sim 10\text{-m-thick}$  layer of pillow lava on the seafloor with a magnetization similar to  $10\text{ A m}^{-1}$ . This pillow lava field likely formed in May–July 1964 through intrusive channeling of basaltic magma through a contemporaneous lava delta.

A clear magnetic anomaly is located on the southern edge of the submarine mound that is the remnant of the ephemeral island of Jolnir, formed in 1966. The anomaly correlates with a  $30\text{--}40\text{ m}$  high submarine topographic knob, seen in 1964 bathymetry data and a 1980 seismic profile. The knob apparently pre-dates the formation of Surtsey because surveys of ocean surface temperature, performed during the first days of the eruption in November 1963, did not indicate any heating at this location.

No magnetic anomalies are associated with the submarine mounds that are the remnant of the ephemeral islands of Syrtlingur, formed in 1965, and Jolnir, formed in 1966. In contrast, a weak anomaly is associated with the submarine mound of Surtla, formed in 1963–1964. The data are not conclusive, but the source of this anomaly may be a feeder dyke or a fissure fill of coherent basaltic rocks along the ridge of Surtla.

The differences between the magnetic anomalies for Surtla on one hand and for Jolnir and Syrtlingur on the other, may be due to the eruption of Surtla being of lower explosive intensity. Surtla did not apparently experience the powerful phreatomagmatic explosions

observed at other vents, which produce pyroclastic deposits mainly with weak magnetic properties. Beneath Surtsey and its satellite islands, apparently no sub-seafloor intrusions exist of a scale sufficiently large to generate an anomaly detectable by the aeromagnetic survey. This does not rule out intrusions, but their volume and extent would have to be relatively minor compared to the main bodies causing anomalies in this area. This study indicates that dense magnetic surveying is a useful tool to assess the characteristics of a shallow submarine volcanic field. As such, it provides a reference for identifying past eruption sites and assessing past activity in similar volcanic fields. This approach thus has potential for hazard assessment at islands and coastal settings.

## CRediT authorship contribution statement

**Sara Sayyadi:** Conceptualization, Data curation, Formal analysis, Investigation, Methodology, Project administration, Resources, Software, Supervision, Validation, Visualization, Writing original draft, Writing review & editing. **Magnús T. Gudmundsson:** Funding acquisition, Project administration, Supervision, Validation, Writing review & editing, Conceptualization, Data curation, Methodology. **James D.L. White:** Funding acquisition, Validation, Writing review & editing. **Thorsteinn Jonsson:** Data curation. **Maxwell C. Brown:** Data curation, Writing review & editing. **Marie D. Jackson:** Funding acquisition, Writing review & editing.

## Declaration of competing interest

The authors declare that they have no known competing financial interests or personal relationships that could have appeared to influence the work reported in this paper.

## Data availability

Data will be made available on request.

## Acknowledgments

The work is funded, in part, by a grant of excellence from the Icelandic Research Fund, no 163083-052 (IceSUSTAIN). It also depended critically on the funding obtained through the state-funded volcanic hazard program GOSVA, through the sub-project: Methods to estimate eruption frequency in shallow ocean areas. The surveying would never have been possible without the dedicated work of the pilot and owner of Garðaflug Aviation Company, Úlfar Henningsson. Arni Vesteinsson at the Hydrographic Division of the Icelandic Coast Guard provided a bathymetry map of 1964 and Gunnlaugur Björnsson provided the 1965 Leirvogur Observatory data. The Institute of Earth Sciences paleomagnetism laboratory was funded by the Icelandic Centre for Research (Rannís). JDLW's work with Surtsey has been funded by a University of Otago Research Grant and subcontracts from GNS Science. Thoughtful reviews by two anonymous reviewers substantially improved the quality of this publication.

## Appendix A. Supplementary data

Supplementary data to this article can be found online at <https://doi.org/10.1016/j.jvolgeores.2024.108096>.

## References

Baldursson, S., Ingadóttir, A. (Eds.), 2007. Nomination of Surtsey for the UNESCO World Heritage List.

Blakely, R.J., 1995. Potential Theory in Gravity and Magnetic Applications, 461 pp. Cambridge University Press.

Blanco-Montenegro, I., Ritis, R., Chiappini, M., 2007. Imaging and modelling the subsurface structure of volcanic calderas with high-resolution aeromagnetic data at Vulcano (Aeolian Islands, Italy). *Bull. Volcanol.* 69 <https://doi.org/10.1007/s00445-006-0100-7>.

Blanco-Montenegro, I., Montesinos, F.G., Nicolosi, I., et al., 2020. Three-dimensional magnetic models of La Gomera (Canary Islands): Insights into the early evolution of an Ocean Island Volcano. *Geochem. Geophys. Geosyst.* 21 <https://doi.org/10.1029/2019GC008787> e2019GC008787.

Cassidy, J., France, S.J., Locke, C.A., 2007. Gravity and magnetic investigation of maar volcanoes, Auckland volcanic field, New Zealand. *J. Volcanol. Geotherm. Res.*, 159, 1–3, 153–163.

Cole, P.D., Guest, J.E., Duncan, A.M., Pacheco, J.M., 2001. Capelinhos 1957–1958, Faial, Azores: deposits formed by an emergent surtseyan eruption. *Bull. Volcanol.* 63 <https://doi.org/10.1007/s004450100136>.

Cronin, S.J., Bremna, M., Smith, I.E.M., et al., 2017. New volcanic island unveils explosive past. *Eos (United States)* 98. <https://doi.org/10.1029/2017eo076589>.

Finn, C.A., Morgan, L.A., 2002. High-resolution aeromagnetic mapping of volcanic terrain, Yellowstone National Park. *J. Volcanol. Geotherm. Res.* 115 [https://doi.org/10.1016/S0377-0273\(01\)00317-1](https://doi.org/10.1016/S0377-0273(01)00317-1).

Geometrics, Inc., 2019. MagArrow Magnetometer Manual. Rev B. <https://www.geometrics.com/product/magarrow/>.

Geosoft, 2022. GM-SYS 3D Software [Computer Software]. Geosoft Inc.. Available from. <https://www.seequent.com/products-solutions/geosoft-oasis-montaj/>

Geosoft Inc., 2015. Defining and Applying Filters and Inverse FFT in MAGMAP. <https://www.seequent.com/products-solutions/geosoft-oasis-montaj/>.

Golden Software, 2021. Surfer. <https://www.goldensoftware.com/products/surfer>.

Gudmundsson, M.T., Milsom, J., 1997. Gravity and magnetic studies of the subglacial Grímsvötn volcano, Iceland: Implications for crustal and thermal structure. *J. Geophys. Res. Solid Earth* 102, 7691–7704. <https://doi.org/10.1029/96JB03808>.

Gunnarsson, K., Egilson, T., Hafstad, T., et al., 2005. Bergrunnsskonnénum a hugsanlegrí jarðgangaleið milli lands og Eyja. *Bylgjubrots- og flugseglumálinagar* og athugun a gognum ír borholum. (In Icelandic: Study of the bedrock along a possible path of a road tunnel between mainland Iceland and Vestmannaeyjar. Results from Refraction and Aeromagnetic Surveys and Data from drillholes) (ISOR-2005/033 45 pp).

Hoskuldsson, A., Oladóttir, B., Larsen, G., Gudmundsson, M.T., 2015. *Vestmannaeyjar. In: Catalogue of Icelandic volcanoes*. IMO, UI and CPD-NCIP.

Jackson, M.D., Gudmundsson, M.T., Weisenberger, T.B., et al., 2019. SUSTAIN drilling at Surtsey volcano, Iceland, tracks hydrothermal and microbiological interactions in basalt 50 years after eruption. *Sci. Drill.* 25, 35–46. <https://doi.org/10.5194/sd-25-35-2019>.

Jackson, M.D., Heap, M.J., Vola, G., Ardit, M., Rhodes, J.M., Peterson, J.G., Tamura, N., Gudmundsson, M.T., 2024. Material and mechanical properties of Young Oceanic Basalt, Surtsey Volcano, Iceland. *Geol. Soc. Am. Bull.* <https://doi.org/10.1130/B37037.1>.

Jakobsson, S.P., 1979. Petrology of recent basalts of the eastern volcanic zone, Iceland. *Acta Naturalia Islandica* 26, 1–103.

Jakobsson, S.P., Moore, J.G., 1982. The Surtsey drilling project of 1979. *Res. Progr. Report* 9, 76–93.

Jakobsson, S.P., Gudmundsson, G., Moore, J.G., 2000. Geological monitoring of Surtsey, Iceland 1967–1998. *Surtsey Res.* 11, 99–108.

Jakobsson, S.P., Thors, K., Vesteinsson, Ath., Ashbjornsdóttir, L., 2009. Some aspects of the seafloor morphology at Surtsey volcano: the new multibeam bathymetric survey of 2007. *Surtsey Res.* 12, 9–20.

Kaneko, T., Yasuda, A., Shimano, T., et al., 2005. Submarine flank eruption preceding caldera subsidence during the 2000 eruption of Miyakejima Volcano, Japan. *Bull. Volcanol.* 67 <https://doi.org/10.1007/s00445-004-0407-1>.

Kokelaar, B.P., 1983. The mechanism of Surtseyan volcanism. *J. Geol. Soc. Lond.* 140, 939–944. <https://doi.org/10.1144/gsjgs.140.6.0939>.

Kokelaar, B.P., 1986. Magma-water interactions in subaqueous and emergent basaltic. *Bull. Volcanol.* 48 <https://doi.org/10.1007/BF01081756>.

Kokelaar, B.P., Durant, G.P., 1983. The submarine eruption and erosion of Surtla (Surtsey), Iceland. *J. Volcanol. Geotherm. Res.* 19 [https://doi.org/10.1016/0377-0273\(83\)90112-9](https://doi.org/10.1016/0377-0273(83)90112-9).

Kristjansson, L., 1970. Paleomagnetism and magnetic surveys in Iceland. *Earth Planet. Sci. Lett.* 8 [https://doi.org/10.1016/0012-821X\(70\)90158-5](https://doi.org/10.1016/0012-821X(70)90158-5).

Kristjansson, L., 1982. Geomagnetic polarity mapping of Icelandic lavas: comparison with ocean-floor magnetic lineations. *Earth Evol. Sci.* 2, 126–129.

Kristjansson, L., 2013. The Stardalur magnetic anomaly, SW-Iceland: a review of research in 1968–2012. *JOKULL* 63, 1–16.

Lefebvre, N.S., White, J.D.L., Kjarsgaard, B.A., 2012. Spatter-dike reveals subterranean magma diversions: Consequences for small multivent basaltic eruptions. *Geology* 40. <https://doi.org/10.1130/G32794.1>.

Malmborg, S.-A., 1965. A report on the temperature effect of the Surtsey eruption on the sea water. *Surtsey Res. Progr. Report* 1, 6–9.

Mattsson, H., Hoskuldsson, A., 2003. Geology of the Heimaey volcanic Centre, South Iceland: early evolution of a central volcano in a propagating rift? *J. Volcanol. Geotherm. Res.* 127, 55–71. [https://doi.org/10.1016/S0377-0273\(03\)00178-1](https://doi.org/10.1016/S0377-0273(03)00178-1).

McPhie, J., White, J.D.L., Gorni, C., et al., 2020. Lithofacies from the 1963–1967 Surtsey eruption in SUSTAIN drill cores SE-2a, SE-2b and SE-03. *Surtsey Res.* 14, 19–32. <https://doi.org/10.33112/surtsey.14.2>.

Moore, J.G., 1985. Structure and eruptive mechanisms at Surtsey Volcano, Iceland. *Geol. Mag.* 122, 649–661. <https://doi.org/10.1017/S0016756800032052>.

Mushayandebvu, M.F., van Driel, P., Reid, A.B., Fairhead, J.D., 2001. Magnetic source parameters of two-dimensional structures using extended Euler deconvolution. *Geophysics* 66. <https://doi.org/10.1190/1.1444971>.

Okuma, S., Stötter, C., Supper, R., et al., 2009. Aeromagnetic constraints on the subsurface structure of Stromboli Volcano, Aeolian Islands, Italy. *Tectonophysics* 478. <https://doi.org/10.1016/j.tecto.2009.02.035>.

Oskarsson, B.V., Jonasson, K., Valsson, G., Belart, J.M.C., 2020. Erosion and sedimentation in Surtsey island quantified from new DEMs. *Surtsey Res.* 14, 67–73. <https://doi.org/10.33112/surtsey.14.5>.

Paoletti, V., Supper, R., Chiappini, M., et al., 2009. Aeromagnetic survey of the Somma-Vesuvius volcanic area. *Ann. Geophys.* 48 <https://doi.org/10.4401/ag-3196>.

Parker, R.L., 1972. The rapid calculation of potential anomalies. *Geophys. J. R. Astron. Soc.* 42, 315–334.

Re, G., White, J.D.L., Muirhead, J.D., Ort, M.H., 2016. Subterranean fragmentation of magma during conduit initiation and evolution in the shallow plumbing system of the small-volume Jagged Rocks volcanoes (Hopi Buttes Volcanic Field, Arizona, USA). *Bull. Volcanol.* 78 <https://doi.org/10.1007/s00445-016-1050-3>.

Reid, A.B., Allsop, J.M., Granser, H., et al., 1990. Magnetic interpretation in three dimensions using Euler deconvolution. *Geophysics* 55, 81–90. <https://doi.org/10.1190/1.1442774>.

Rivera, J., Lastras, G., Canals, M., et al., 2013. Construction of an oceanic island: Insights from the El Hierro (Canary Islands) 2011–2012 submarine volcanic eruption. *Geology* 41. <https://doi.org/10.1130/G33863.1>.

Sayyadi, S., Einarsson, P., Gudmundsson, M.T., 2021. Seismic activity associated with the 1963 1967 Surtsey eruption off the coast of South Iceland. *Bull. Volcanol.* 83 <https://doi.org/10.1007/s00445-021-01481-0>.

Sayyadi, S., Gudmundsson, M.T., Einarsson, P., 2022. Volcanic tremor associated with the Surtsey eruption of 1963 1967. *Jokull* 72, 21–34.

Schopka, H.H., Gudmundsson, M.T., Tuffen, H., 2006. The formation of Helgafell, a monogenetic subglacial hyaloclastite ridge: Sedimentology, hydrology and volcano-ice interaction. *J. Volcanol. Geotherm. Res.* 152, 359–377.

Sigtryggsson, H., Sigurdsson, E., 1966. Earth tremors from the Surtsey eruption 1963–1965. *Surtsey Res. Progr. Report II*, 131–138.

Sigurdsson, I.A., Jakobsson, S.P., 2006. Evolution of the Vestmannaeyjar volcanic system. *Geochim. Cosmochim. Acta* 70, A590. <https://doi.org/10.1016/J.GCA.2006.06.1095>.

Sigurgeirsson, T., 1966. Geophysical measurements in Surtsey carried out during the year of 1965. *Surtsey Res. Progr. Report II*, 181–185.

Sigurgeirsson, T., 1968. Continued geomagnetic and seismic measurements on Surtsey. *Surtsey Res. Progr. Report SIV*, 173–175.

Somoza, L., Gonzalez, F.J., Barker, S.J., et al., 2017. Evolution of submarine eruptive activity during the 2011–2012 El Hierro event as documented by hydroacoustic images and remotely operated vehicle observations. *Geochem. Geophys. Geosyst.* 18 <https://doi.org/10.1002/2016GC006733>.

Spector, A., Grant, F.S., 1970. Statistical models for interpreting aeromagnetic data. *Geophysics* 35, 293–302. <https://doi.org/10.1190/1.1440092>.

Tada, N., Ichihara, H., Nakano, M., et al., 2021. Magnetization structure of Nishinoshima volcano, Ogasawara Island arc, obtained from magnetic surveys using an unmanned aerial vehicle. *J. Volcanol. Geotherm. Res.* 419, 107349 <https://doi.org/10.1016/J.JVOLGEORES.2021.107349>.

Thorarinsson, S., 1965. The Surtsey eruption: Course of events and the development of the new island. *Surtsey Res. Progr. Report I*, 51–55.

Thorarinsson, S., 1966. The Surtsey eruption course of events and the development of Surtsey and other new islands. *Surtsey Res. Progr. Report II*, 117–123.

Thorarinsson, S., 1967a. The Surtsey eruption and related scientific work. *Polar Record* 13, 571–578. <https://doi.org/10.1017/S0032247400058113>.

Thorarinsson, S., 1967b. The Surtsey eruption. Course of events during the year 1966. *Surtsey Res. Progr. Report III*, 84–90.

Thorarinsson, S., 1967c. Surtsey, the New Island in the North Atlantic. Viking Press, New York, pp. 1–47.

Thorarinsson, S., 1968a. The last phases of the Surtsey eruption [Síðustu ættir Eyjaelda] (in Icelandic with English summary). *Naturfraeindurinn* 38, 113–135.

Thorarinsson, S., 1968b. The Surtsey eruption - course of events during the year 1967. *Surtsey Res. Prog. Rep. IV*, 143–149.

Thorarinsson, S., Einarsson, T., Sigvaldason, G., Elisson, G., 1964. The submarine eruption off the Vestmann islands 1963–64 - a preliminary report. *Bull. Volcanol.* 27, 435–445. <https://doi.org/10.1007/BF02597544>.

Thors, K., Helgason, J., 1988. Jarðlog við Vestmannaeyjar. *Afangaskýrsla um jarðlagagreiningu og konunn neðansjávareldvarpa með endurvarpsmaelingum*. (in Icelandic: Stratigraphy around Vestmannaeyjar. A Progress Report on Analysis and Exploration of Submarine Volcanic Structure from Seismic Reflection). *Hafrannsoknastofnun*, 41.

Thors, K., Jakobsson, S.P., 1982. Two seismic reflection profiles from the vicinity of Surtsey, Iceland. In: *Surtsey Research Progress Report IX*, pp. 149–151.

Tomasson, J., 1967. On the origin of sedimentary waters beneath Vestmann Islands. *Jokull* 1, 300–311.

Ueda, Y., 2007. A 3D magnetic structure of Izu-Oshima Volcano and their changes after the eruption in 1986 as estimated from repeated airborne magnetic surveys. *J. Volcanol. Geotherm. Res.* 164 <https://doi.org/10.1016/j.jvolgeores.2007.04.017>.

Veststeinsson, A., 2009. Surveying and charting the Surtsey area. *Surtsey Res.* 12, 49–53.

Walker, G.P.L., 2000. Basaltic volcanoes and volcanic systems. In: *Encyclopedia of Volcanoes*.

Watton, T.J., Jerram, D.A., Thordarson, T., Davies, R.J., 2013. Three-dimensional lithofacies variations in hyaloclastite deposits. *J. Volcanol. Geotherm. Res.* 250 <https://doi.org/10.1016/j.jvolgeores.2012.10.011>.

Weisenberger, T.B., Gudmundsson, M., et al., 2019. Operational Report for the 2017 Surtsey Underwater Volcanic System for Thermophiles, Alteration Processes and INnovative Concretes (SUSTAIN) Drilling Project at Surtsey Volcano, Iceland, pp. 1–240.

Weisenberger, T.B., Gudmundsson, M.T., Gunnarsson, B.S., et al., 2022. Measurements of the inclination of the SE-03 Borehole on Surtsey Volcano. In: *Surtsey Report*, 15.

White, J.D.L., 1996. Pre-emergent construction of a lacustrine basaltic volcano, Pahvant Butte, Utah (USA). *Bull. Volcanol.* 58 <https://doi.org/10.1007/s004450050138>.

White, J.D.L., Schipper, C.I., Kano, K., 2015. Submarine explosive eruptions. In: *The Encyclopedia of Volcanoes*.